Journal of Physics: Conference Series

PAPER • **OPEN ACCESS**

Comparison of horizontal wind speed and direction measurements from dual-Doppler radar and profiling lidars

To cite this article: A L Vöhringer *et al* 2024 *J. Phys.: Conf. Ser.* **2767** 092101

Journal of Physics: Conference Series **2767** (2024) 092101 doi:10.1088/1742-6596/2767/9/092101

Comparison of horizontal wind speed and direction measurements from dual-Doppler radar and profiling lidars

A L Vöhringer[1,2], J Gottschall[3], B D Hirth[4,5], L-Y Hung[3], J K Lundquist[6,7], J Schneemann[1,2], J L Schroeder[4,5], F Theuer[1,2], M Kühn[1,2]

[1]Carl von Ossietzky Universität Oldenburg, School V, Institute of Physics
[2]ForWind - Center for Wind Energy Research, Küpkersweg 70, 26129 Oldenburg, Germany
[3]Fraunhofer Institute for Wind Energy Systems IWES, Bremerhaven, Germany
[4]Texas Tech University, Lubbock, TX, USA
[5]SmartWind Technologies, LLC, Lubbock, TX, USA
[6]University of Colorado Boulder, Boulder, CO, USA
[7]National Renewable Energy Laboratory, Golden, CO, USA

E-mail: `lilen.voehringer@uni-oldenburg.de`

Abstract. Dual-Doppler radar is a relatively new technology in the wind energy community and thus not yet studied vastly. This paper aims to compare horizontal wind speed and direction data retrieved from dual-Doppler radar and profiling lidars within the American WAKE experimeNt (AWAKEN) to investigate the influence of measurement height, wind direction and speed on the comparison. The 10-min averaged data show a better agreement of the measurements for higher altitudes, especially at faster wind speeds. For the wind direction, two sectors of larger differences in the measurements were detected: around 270° transient winds occur with a higher frequency than in other sectors. To explain the different measurement values in the wind direction sector around 90°, further studies, e.g. on the influence of atmospheric stability, are necessary.

1. Introduction

Remote sensing techniques such as Doppler lidar and radar are becoming ever more important in wind energy. Compared to expensive meteorological masts, remote sensing maintains several advantages such as mobility, the ability to scan vast areas instead of single points, and the capability to assess wind speeds along the beam [1]. Various configurations of beam geometries can be used to retrieve 2D or 3D wind vectors [2], while dual-Doppler (DD) radar offers the possibility to retrieve these velocities over a very large area [3]. Compared to lidars, the wind radar technology provides fine spatial resolution along the beam as well as a very fast scan speed [4]. However, the wind radar beam is not collimated, as lidar beams are, and diverges with an opening angle of 0.5° [5], increasing the probe volume perpendicular to the beam with further distance.

As the synthesis of measurements from multiple radars is a relatively new application in wind energy, it has not yet been studied as extensively as lidars. It is thus important to examine the resulting synthesized measurements of horizontal wind from radar technology to evaluate these new devices. Given the recent advent of radar in wind energy, very few long-duration data sets are available for validation. However, one data set was collected in the American WAKE

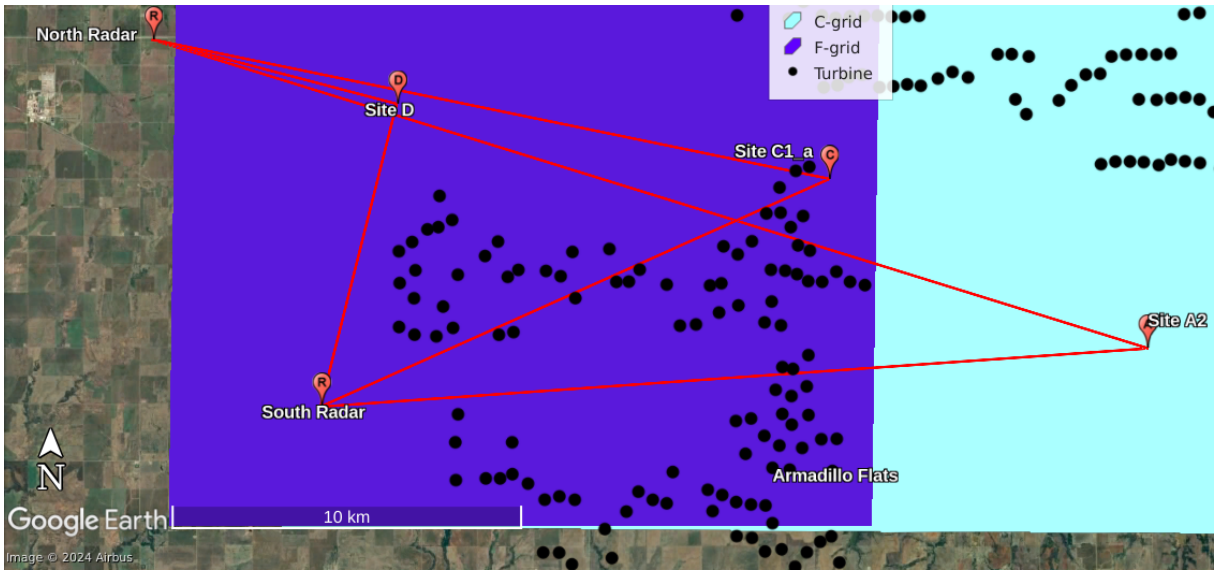

Figure 1. Map of the AWAKEN measurement site focusing on the radar and lidar (sites D, C1a and A2) positions of the devices used for this study. Moreover, the coverage of the fine (F) and the coarse (C) grid over the lidar positions is shown, as well as the turbine positions (black dots). Please note, that the C-grid also covers the area of the F-grid. For visualization, the red lines connect the radars with each lidar site.

experimeNt (AWAKEN) [6], where three profiling lidars using a Doppler Beam Swing (DBS) [7] scanning strategy are located within the measurement domain of two X-band wind radars.
This paper aims to compare the horizontal wind speed and wind direction retrieved from the DD radar system with these three profiling lidars to better understand the effects of the devices' different measurement strategies on the retrieved wind vectors. The focus lies on investigating the influence of different measurement heights and wind directions on the comparison.

2. Methodology

The AWAKEN campaign is a large project lead by the National Renewable Energy Lab (NREL). The measurement site is located in Oklahoma and the terrain is relatively flat. Even though this campaign comprises many instruments and research goals, in the following, we will focus only on the aspects relevant for this study. For further information including a long-term wind rose of the site, please see [6]. The data used here was collected from June 1st 2023 until September 16th 2023. The profiling lidars are positioned at different distances from the X-band radar devices, as shown in Figure 1. The exact distances are listed in Table 1. Neither met mast nor SCADA data, and thus no information about turbine wakes, was available at the time of this publication.
The X-band radars have a probe volume length of 9 m along the beam. Perpendicular to the beam, the probe volume increases with distance, as the radar beam diverges with an opening angle of 0.5°. At the farthest distance used in this study, namely at site A2, the vertical extension of the north radar's probe volume amounts to roughly 258 m. Each radar scans at 30 °/s on 18 different elevations. Covering an azimuthal sector of 140° at each elevation, a volumetric scan takes approximately 2 min. The line-of-sight measurements of the radars are processed by SmartWind Technologies' software to reconstruct a 2D horizontal wind field on a coarse (C) and fine (F) Cartesian grid: Prior to grid interpolation, the raw polar data go through a general quality assurance process where the various radar moments are leveraged to threshold out potentially erroneous velocity measurements e.g. associated with ground clutter or non-meteorological targets such as buildings and trees. The objective analysis scheme used

to interpolate the radar data from their native polar coordinate space onto both Cartesian grids first makes use of a nearest neighbor search where for the fine (course) grid, the 15 (25) closest radar bins are considered. For those collections of candidate radar values, a radius of influence (ROI) that increases linearly with radar range is implemented. Between ranges of 1.5 km and 35 km, a ROI of 10 m to 200 m is used in the horizontal and 5 m to 75 m is used in the vertical. A Barnes (exponential) weight function is then applied to radar bins that lie within the ROI for each Cartesian grid point. The F-grid uses a 25 m horizontal grid spacing while the C-grid covers a larger area using a 50 m horizontal grid spacing. Moreover, the F-grid only includes locations, where the radar beams meet at an angle of at least 30°, whereas the C-grid also includes locations where the radar beams meet at angles down to 20°. Both grids are available at ten altitudes above mean sea level between 375 m to 625 m in vertical steps of 25 m, aiming to cover the rotor area of several wind turbines in the measurement domain. These heights were transformed to the respective heights above ground level at each lidar site by subtracting the elevation of the respective lidar, as listed in Table 1. All evaluation steps described below were performed for both grids, except at site A2, as this lidar site is out of the reach of the F-grid.
The profiling lidars are Vaisala WindCubes v1 (sites C1a and A2) and a WindCube v2.0 (site D). They follow a 4-beam scan strategy, where they measure to each cardinal direction in an opening angle of approximately 28°. Additionally, the lidar closest to the radars (site D) also measures vertically upwards. With the DBS strategy, each lidar calculates the wind speed and direction at several measurement heights between 40 m and 220 m in steps of 20 m above their respective elevation. Additionally, the lidar at site D uses steps of 10 m until a height of 100 m and is set to a maximal height of 200 m. Due to the cone angle of 28°, the opposing measurement points, from which the wind vectors are calculated, have a horizontal distance of approximately 38 m at a measurement height of 40 m, and a horizontal distance of approximately 188 m at a measurement height of 200 m. It takes roughly 4 s to measure the line-of-sight data along the 4/5 beams. The WindCube software automatically calculates the 10-min average. For sites A2 and C1a, the 2 min average is also calculated by the WindCube software.
As the measurement time scales of both systems differ, all data was assembled to 10-min average values, following wind industry standards. We used a threshold of 80 % data availability for each 10 min interval. The radar software already includes a data filter, whereas the lidar data was filtered for its carrier to noise ratio (CNR) with values of $-22\,\mathrm{dB} < \mathrm{CNR} < 0\,\mathrm{dB}$ retained. All cases with wind speeds below 5 m/s were excluded to avoid large fluctuations in wind direction. For the comparison, the closest radar grid point to the lidar position was selected. Depending on the comparison location, the horizontal separation between the lidar position and the radar grid point was between 11 m to 27 m.
Finally, the measurements were linearly interpolated in height to the measurement height of the respective other device. The linear interpolation was chosen as a simple approach and we assume it is justified as the vertical measurement density is relatively high with max. 25 m spacing. To investigate secondary influences, the data was binned for measurement heights in steps of 50 m, horizontal wind speed in steps of 5 m/s and wind direction in bins of 10°. For this study we considered only bins with at least 10 samples.

3. Results

In this section, we analyse the correlation plots of all collected data. Afterwards, we examine the results binned by height and wind speed or direction. Finally, we investigate the influence of transient winds on the comparison of the radar and lidar data.

3.1. Correlation over all heights

The correlation plots for the different lidar sites and radar grids are shown in Figure 2 and 3 for the horizontal wind speed v_{hor} and direction ϕ, respectively. The fit parameters as well as the

Table 1. Geometrical parameters influencing the lidar-radar comparison resulting from the geographical positions of the lidars and radars.

Lidar Site	Distance to south radar	Distance to north radar	Approx. angle between radar beams	Distance to nearest F-grid point	Distance to nearest C-grid point	Elevation [m ASL]
D	8.8 km	7.2 km	90°	15.32 m	17.83 m	343 m
C1a	15.8 km	19.6 km	35°	11.54 m	19.74 m	329 m
A2	23.6 km	29.6 km	20°	-	26.51 m	325 m

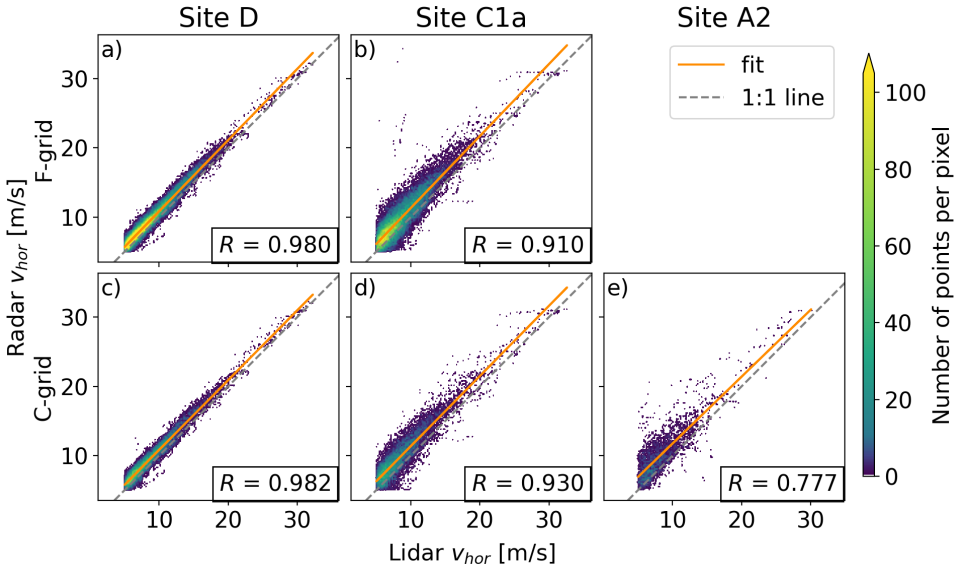

Figure 2. Correlation of the horizontal wind speed v_{hor} over all measurement heights shown for the different lidars (columns), as well as the fine (F) and coarse (C) grid of the radar (rows). The correlation coefficient R is given.

sample sizes are listed in Table 2. The correlation coefficient is best ($R > 0.980$) at site D, where the lidar is closest to the radars and the radar beams meet at an angle of approximately 90°. For larger distances and smaller angles between the radars, the correlation coefficient reduces, until reaching its lowest values (0.777) at the farthest site (A2). The correlation coefficients are slightly higher for the C-grid, as compared to the F-grid. This is not expected, as the F-grid points are always closer to the lidars, than the C-grid points, as shown in Table 1. A possible explanation might result from fewer nearest neighbour points considered for the F-grid in the wind field reconstruction, as opposed to the C-grid. Hence, the wind field reconstruction of the C-grid shows better agreement with the lidar measurements. The correlation coefficient of the F-grid of all aggregated lidar sites (Table 2) is better than of the C-grid, just because site A2 is located outside of the F-grid and thus not included in the correlation.

Horizontal wind speed correlations show a positive offset and a slope larger than 1, meaning that the radar measures faster wind speeds than the lidar. For the wind direction, this offset is site-dependent. For site D, the radar detects slightly larger wind direction values than the lidar while at sites C1a and A2, the offset is negative. Finally, it is interesting to see a larger spread in the correlation plots around wind directions of 90° and 270°. This variability will be further investigated in Section 3.4.

For brevity reasons, in the upcoming sections, we focus on the results of the F-grid at all available lidar sites (D and C1a), as the results for the C-grid are very similar but sometimes distorted

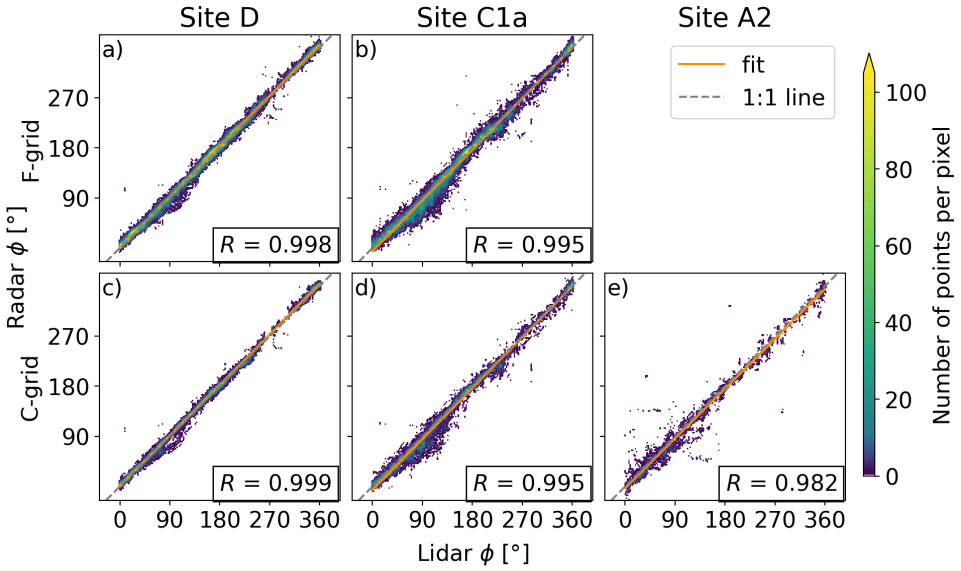

Figure 3. Correlation of the wind direction ϕ over all measurement heights shown for the different lidars (columns), as well as the fine (F) and coarse (C) grid of the radar (rows). The correlation coefficient R is given.

due to the larger deviations at site A2.

Table 2. Fit parameters, correlation coefficient and sample size (N) for the correlation plots of the horizontal wind speed v_{hor} and wind direction ϕ.

		F-grid				C-grid			
	Lidar Site	Corr. coeff. R	Fit slope	Fit offset	N	Corr. coeff. R	Fit slope	Fit offset	N
v_{hor}	D	0.980	1.028	0.55 m/s	34,248	0.982	1.008	0.74 m/s	13,336
	C1a	0.910	1.039	0.92 m/s	30,190	0.930	1.014	1.22 m/s	11,372
	A2	–	–	–	–	0.777	0.966	2.08 m/s	3,523
	all	0.945	1.031	0.75 m/s	64,438	0.932	1.001	1.14 m/s	28,231
		F-grid				C-grid			
	Lidar Site	Corr. coeff. R	Fit slope	Fit offset	N	Corr. coeff. R	Fit slope	Fit offset	N
ϕ	D	0.988	1.012	0.13°	34,248	0.999	1.009	0.65°	13,336
	C1a	0.995	1.017	−5.84°	30,190	0.995	1.016	−6.21°	11,372
	A2	–	–	–	–	0.982	0.993	−2.92°	3,523
	all	0.996	1.015	−2.74°	64,438	0.995	1.011	−2.70°	28,231

3.2. Influence of measurement height and wind speed

Figure 4 shows the mean absolute difference (MAD) of the horizontal wind speed (a) and the correlation for the wind direction (b) of the F-grid data, binned by measurement height and the lidar's horizontal wind speed. The MAD is largest at lower altitudes. For lower altitudes, the MAD increases with wind speed, whereas it decreases with wind speed for higher altitudes. This behaviour can be attributed to more turbulent structures occurring close to the ground, whereas the flow is assumed to be more homogeneous at higher altitudes. This effect is even stronger, for faster wind speeds.

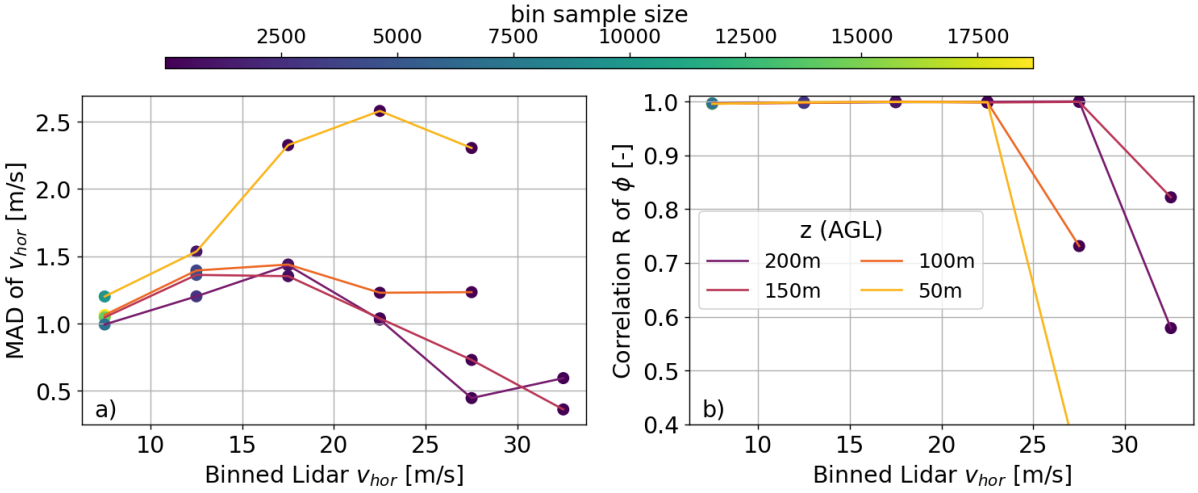

Figure 4. Mean absolute difference (MAD) of horizontal wind speed v_{hor} a) and correlation of wind direction ϕ b) of the lidar data from sites D and C1a with the F-grid data binned for wind speed and height. The marker colour represents the bin's sample size.

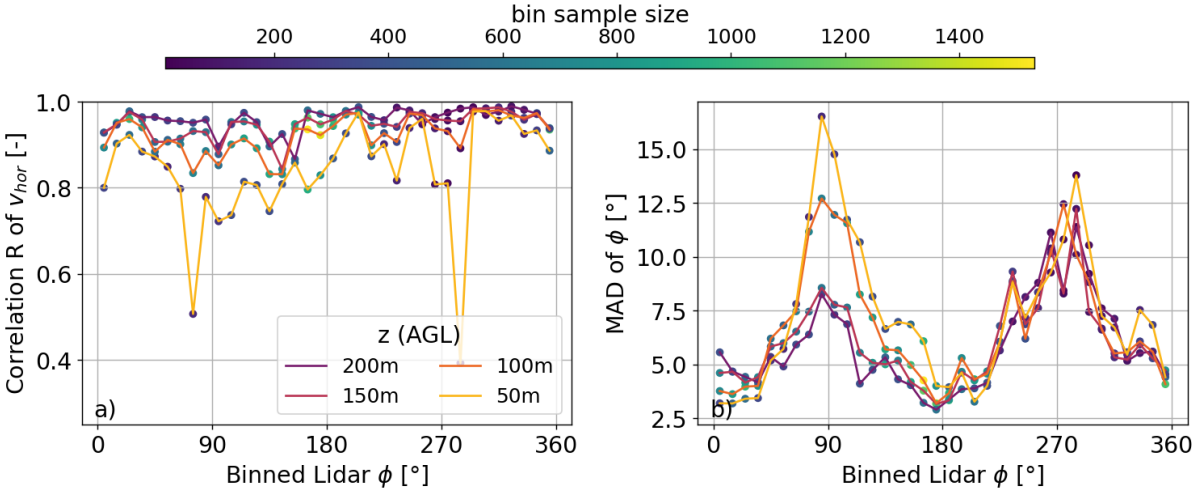

Figure 5. Correlation of horizontal wind speed v_{hor} a) and mean absolute difference (MAD) of wind direction ϕ b) of the lidar data from sites D and C1a with the F-grid data binned for wind direction and height. The marker colour represents the bin's sample size.

The correlation of the wind direction does not show any strong dependencies with height. The smaller wind direction correlation values at the largest wind speeds can mainly be attributed to smaller sample sizes within those bins. Similar observations can be found in the C-grid data (not shown).

3.3. Influence of measurement height and wind speed

The comparison of the radar and lidar data when binned by wind direction and height for the F-grid is shown in Figure 5. The wind speed correlations are good ($R > 0.8$) for all measurement heights above 400 m, except for the wind direction bin of 155° at 550 m height. For the highest altitudes, the correlation of most wind direction bins shows good agreement reaching coefficients close to 1.0. For lower measurement heights, the correlation coefficients are slightly lower in most wind direction bins. Only the wind direction bins around 90° and 270° show larger differences between the measurement heights, as the correlation coefficients of low altitudes drop below 0.7, while the correlation coefficients of higher altitudes are still between 0.87 and 1.0. A similar

behaviour occurs for the MAD of the wind direction, which shows good agreement ($< 7.5°$) for several wind direction bins and heights. However, deviations increase around 90°, especially at lower measurement heights. Around wind directions of 270° the MAD increases up to 13° for all measurement heights. This wind direction sector contains fewer samples, as it is not prevalent at the measurement site.
One possible explanation for the larger MAD around 90° and 270° could be that the data from those wind directions were collected during transient wind direction events, that might have been detected differently by both devices. To further investigate this, a comparison of higher temporal resolution data will be explored in section 3.4.

3.4. Transient wind direction sectors

To investigate whether the larger deviations for wind directions around 90° and 270° result from changing wind directions, we calculated the wind direction changing rate $\mathrm{d}\phi/\mathrm{d}t$ over 10 minutes, i.e. we calculated the absolute difference in wind direction of two subsequent 10 min values, as detected by the lidar. The occurrence of these wind direction changes is shown for the different wind direction sectors in Figure 6. Most measured cases comprise low changing rates below 25°/10 min. Yet, there are a few larger changing rates, that might lead to larger differences between the radar and lidar measurement, as they might be detected with a temporal shift.
In Figure 7 we show the MAD for the horizontal wind speed and direction when binning for height and wind direction changing rate in 5°/10 min intervals. As before, only bins with at least 10 data points are shown. The changing rate does not affect the MAD of v_{hor} negatively, as the MAD is initially reduced for increasing $\mathrm{d}\phi/\mathrm{d}t$. For larger $\mathrm{d}\phi/\mathrm{d}t$ around 40°/10 min, the MAD increases slightly but does not exceed the initial values of 2.5°/10 min. This is different for the wind direction. The MAD of ϕ initially increases with $\mathrm{d}\phi/\mathrm{d}t$ until approximately 30°/10 min. For larger $\mathrm{d}\phi/\mathrm{d}t$, the MAD varies, which can be attributed to smaller sample sizes. Hence we conclude, that transient winds can influence the MAD of ϕ.
To check, whether transient winds explain the differences in the wind direction sectors around 90° and 270°, we calculated the percentage of transient wind events per wind direction bin. To this end, we classified all wind direction changing rates above 25°/10 min as transient winds (Figure 6). The percentage of transient winds is high for wind directions around 270° and might thus explain the deviations in the radar and lidar measurements.
However, around 90° the percentage of transient wind events is rather low and can thus not explain the different measurements of the radar and lidar in this wind direction sector.
Another possible reason for the deviations in the radar and lidar measurements might result from the atmospheric stability, as this can influence the turbulent structures which might be detected differently by the radar and lidar, due to their different probe volume sizes and geometries. We will present our initial findings on the influence of atmospheric events using an example time series from 2023-06-10 at site C1a (Figure 8), where the wind speed increases with time at higher altitudes. This increase in wind speed is well captured by the radar and observed at all altitudes. Both devices detect some wind direction veer, especially until 03:25 UTC. Towards the end of the time series, the veer reduces, especially as measured by the lidar. Moreover, a low level jet (LLJ) is detected by the lidar, which is most prominent around 03:30 UTC. This LLJ is not seen by the radar. Thus, we conclude that LLJs could affect the radar and lidar data differently and lead to different wind vector values.
Further investigations on the effect of the atmospheric stability are needed to evaluate its influence on the comparison of lidar and radar data.

4. Discussion

The correlation plots showed good agreement ($R > 0.777$) for all lidar sites. The further away the lidar site from the radars, the lower the correlation coefficients. This reduction of the

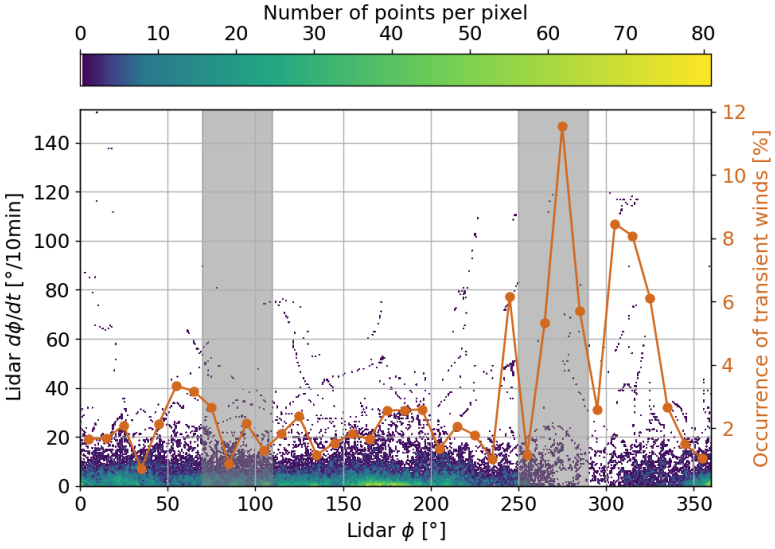

Figure 6. Occurrence of wind direction changing rates $\mathrm{d}\phi/\mathrm{d}t$ of the F-grid (sites D and C1a) for the different wind directions ϕ. The colour represents the data density. The grey areas represent the sectors where the correlation of lidar and radar data showed larger differences. Moreover, the orange line shows the percentage of transient winds with $\mathrm{d}\phi/\mathrm{d}t > 20°/10\,\mathrm{min}$ for each 10° bin of the lidar wind direction.

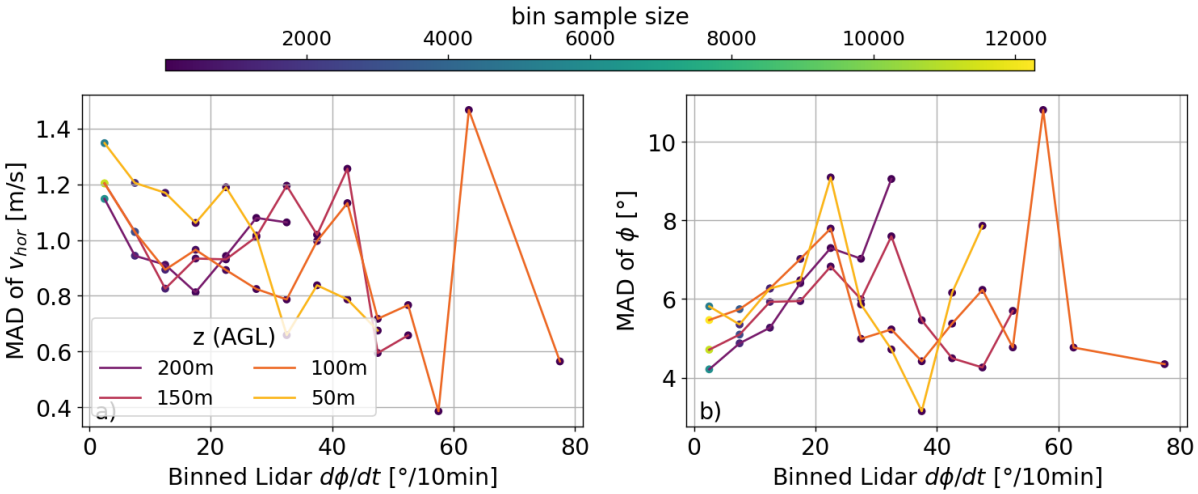

Figure 7. Mean absolute difference (MAD) for the horizontal wind speed v_{hor} a) and direction ϕ b) of the F-grid (sites D and C1a) over binned wind direction changing rate $\mathrm{d}\phi/\mathrm{d}t$. The colours represent the measurement height.

correlation coefficient could result from the radar probe volume increasing with distance to the radars and thus, leading to a vertically larger probe volume at larger distances and thus, a larger uncertainty. Another influence could arise from the angle between the radars. The smaller this angle, the larger the uncertainty in resolving the wind direction and thus, calculating the wind speed. Further studies, e.g. with lidars positioned at the same angle between the radar beams, but at different distances, are necessary to separate the influence of these parameters.

It was not expected to find higher correlation coefficients for the C-grid, than for the F-grid. This slight difference could be explained by the different polar to Cartesian grid interpolation schemes. Using the same scheme for both grids could allow to confirm this hypothesis.

Compared to the lidar, the radar overestimates wind speed. This overestimation is also observed in [8] for the line-of-sight measurements, but could not yet be explained. Further measurement campaigns should comprise met mast data to analyse these increased wind speed measurements.

When investigating the influence of the horizontal wind speed and measurement height on the results, we found larger differences between the radar and lidar measurements closer to the ground. We attribute this to inhomogeneous winds which occur more often close to the

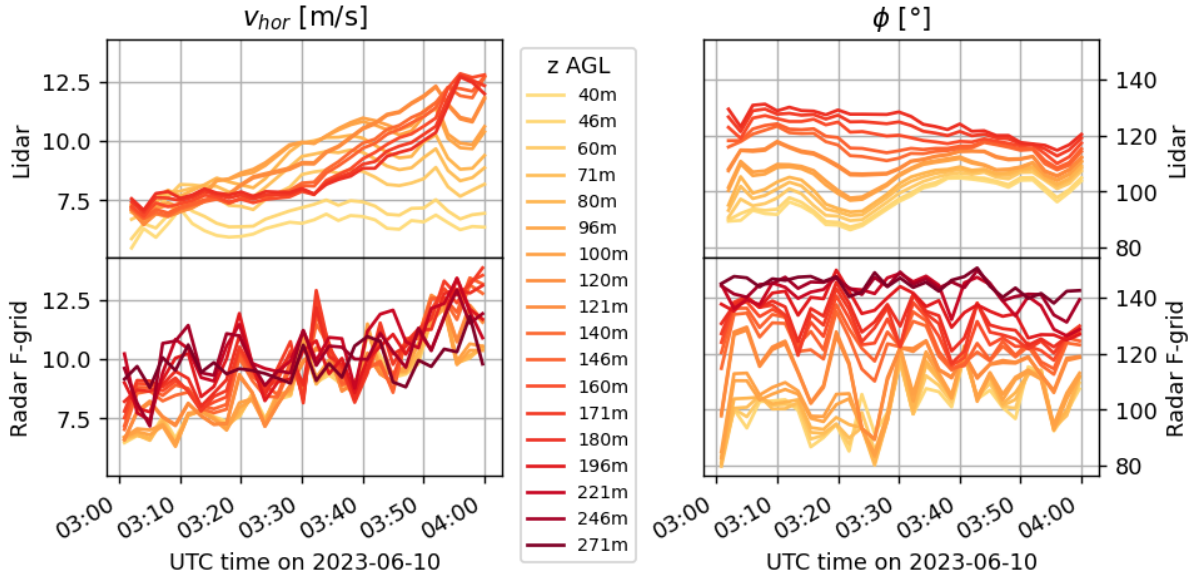

Figure 8. Time series of the horizontal wind speed v_{hor} and direction ϕ of an example situation with wind directions around 90°, where larger deviations were found between radar and lidar data. The data depicted is from site C1a. The temporal resolution is exactly 2 min for the lidar, and approximately 2 min for the radar. The different colours represent the measurement heights above ground level (AGL).

ground. These structures are captured differently by the lidar and radar due to their different measurement scheme and probe volume. While the radar's probe volume increases laterally and vertically with distance, the lidar's DBS cone radius increases with measurement height. Hence, vertical and horizontal turbulence structures are captured differently by the two device types. As these turbulence structures propagate through larger distances when travelling at higher speed, the differences between the radar and lidar data increase at lower altitudes for faster wind speeds.

Similarly, radar and lidar data are most similar at higher altitudes when binning by height and wind direction. The wind direction sectors around 90° and 270° show larger differences at lower altitudes for the horizontal wind speed and direction. Around 270°, also higher altitudes lead to larger differences in the detected wind direction. This was attributed to a higher occurrence of transient wind events in these wind direction sectors. These transient winds seem to be detected differently by the lidar and radar, which could arise from the different measurement strategies or frequencies. As the radars scan over the azimuth sector individually, they each revisit the lidar position approximately every 7 s, however at a different elevation. The lidar on the other hand, takes approximately 1 s to measure along one of its 4 to 5 directions. Under strong wind direction changes the exact measurement time will have a strong impact on the results. Hence, the transient winds could be captured with a slight temporal shift, leading to a larger difference in wind direction.

As the transient wind direction events only explain the differences in the lidar and radar measurements for wind direction sectors around 270°, further investigations of other influencing parameters are necessary to explain the deviations for wind directions around 90°. The deviations in the measurements were strongest at lower altitudes for this wind direction sector. Thus, it is possible that they originate from roughness effects at the surface. When checking the map, however, the terrain around both lidar sides is rather flat and smooth, indicating that the different values at low altitudes do not arise from roughness effects.

Possibly these wind direction sectors contain a larger amount of unstable cases or LLJs, which could influence the radar measurements at far distances stronger, as the probe volume grows

vertically in size, making it more difficult to detect vertical structures as LLJs. Future studies will focus on investigating the influence of atmospheric stability as well as other parameters

5. Conclusion

We compared the radar and lidar derived 10 min averaged values of the horizontal wind speed and direction and investigated the influence of measurement height, wind speed and direction. From the high correlation values we conclude that both techniques measured very similar wind vectors, even though the radar measures faster wind speed values. The closer the lidar to the radar, the better the correlation due to the radar's probe volume increase with distance. This could, however, also result from the angle between the radar beams, which was best for the closest lidar. When binning for height, higher altitudes resulted in better agreement, as the flow is less disturbed relative to closer to the ground. This effect was even larger at faster wind speeds, as wind disturbances advect larger distances under the influence of higher momentum. For the wind direction, larger deviations were found in bins around 90° and 270°. In the latter sector, the percentage of transient wind events is higher than in other sectors, such that the deviations could result from temporally different measurements of the lidar and radar, which has a strong influence in these cases of fast wind direction changes. Further investigations, e.g. of the influence of atmospheric stability, are needed to explain the deviations in the wind direction sector around 90°.

Acknowledgments

We would like to acknowledge the essential contribution of the AWAKEN science team led by the National Renewable Energy Laboratory (NREL) and its institutional and industrial partners. We also thank the NREL-team for their support and helpful discussions of the preliminary results. We acknowledge the support of the technical staff for installing and maintaining the instruments and the landowners from Noble and Garfield counties in Oklahoma for granting access to their land. This work is partly funded by the Federal Ministry for Economic Affairs and Climate Action according to a resolution by the German Federal Parliament in the scope of the research project "Windpark Radar" (Ref.No. 03EE3031B).

References

[1] Letizia S, Zhan L and Iungo G V 2021 *Atmos. Meas. Tech.* **14** 2095–2113
[2] Newsom R K, Berg L K, Shaw W J and Fischer M L 2015 *Wind Energy* **18** 219–235
[3] Nygaard N G and Newcombe A C 2018 *Journal of Physics: Conference Series* **1037** 072008
[4] Ahsbahs T, Nygaard N, Newcombe A and Badger M 2020 *Remote Sensing* **12** ISSN 2072-4292
[5] Valldecabres L, Nygaard N G, Vera-Tudela L, Von Bremen L and Kühn M 2018 *Rem. Sens.* **10** ISSN 2072-4292
[6] Debnath M, Scholbrock A K, Zalkind D, Moriarty P, Simley E, Hamilton N, Ivanov C, Arthur R S, Barthelmie R, Bodini N, Brewer A, Goldberger L, Herges T, Hirth B, Iungo G V, Jager D, Kaul C, Klein P, Krishnamurthy R, Letizia S, Lundquist J K, Maniaci D, Newsom R, Pekour M, Pryor S C, Ritsche M T, Roadman J, Schroeder J, Shaw W J, Dam J V and Wharton S 2022 *J. of Phys.: Conf. Ser.* **2265** 022058
[7] Lundquist J K, Churchfield M J, Lee S and Clifton A 2015 *Atmos. Meas. Tech.* **8** 907–920
[8] Hung L Y, Gottschall J, Vöhringer A L, Hirth B D and Schroeder J L 2024 Comparison of line-of-sight wind speed measurements from an x-band radar and a long-range scanning lidar